

Thermoelectric properties and power generation of a p-Ca₃Co₄O₉/n-CaMnO₃ module

Weerasak Somkhunthot*, Wattanapong Swang, Acharee Tunkasikit

Physics Department, Faculty of Science and Technology, Loei Rajabhat University, 234 Moo 11, Loei-Chiangkan Road, Amphoe Muang, Loei 42000, (THAILAND)

E-mail: weerasak1963@yahoo.co.th

Received: 19th December, 2010 ; Accepted: 29th December, 2010

ABSTRACT

An oxide thermoelectric module has been designed and constructed for electrical power generation. The device composed of thirty-one pairs of p-Ca₃Co₄O₉ and n-CaMnO₃ bulks, ceramic plates, and copper electrodes. Dimensions of both oxide legs were 2.0 mm thick and high and 1.0 mm wide, which were made from powder precursors, obtained from the solid state reaction method. The ceramic plates possessing dimensions 24.5 mm wide and long and 1.0 mm thick were used as substrate. The copper sheets 1.0 mm in width, 2.0 mm length, and 0.05 mm in thickness were attached onto the ceramic plates using epoxy adhesive to maintain achieve electrical conduction. The p-n legs and copper sheets on the ceramic plates were adhered by silver paint. For the measurements of thermoelectric properties at room temperature in air, both bulks showed the low Seebeck coefficient, high electrical resistivity, and large thermal conductivity, which lead to a low power factor and figure of merit. For the preliminary test, the module was used for thermoelectric power generation. The result shows linear dependence between the thermoelectric voltage and temperature difference. This device could generate up to 50 mV of open circuit voltage at hot-side temperature of 423 K and cold-side temperature of 343 K. The internal resistance of the module reached a value of 968.45 kΩ. However, the module built could be used to generate low thermoelectric power. The doped metals have been expected to be one of the candidates for good thermoelectric generators. This will be further investigated.

© 2011 Trade Science Inc. - INDIA

KEYWORDS

Thermoelectric properties;
Thermoelectric generators;
Thermoelectric module.

INTRODUCTION

Up to now, fossil fuels have been the main energy resource of the world. About 80-90% of primary energy needs has been supplied by oil, coal, natural gas, and oil shale^[1]. These energy resources remain of im-

portance in the future. However, these energy resources are non-renewable and cause problems to the environment. This has been a driving force to look for alternative energy resources which are clean, safe, and in the long-term reliable. Thermoelectricity is one of the renewable energy resources that has been widely investi-

Full Paper

gated and is expected to be feasible in the near future. Furthermore, it is a clean form of energy generation, since it can directly convert heat to electrical energy by using non-polluting thermoelectric devices. These are reasons for the growing interest in further research and development of thermoelectric technology.

Thermoelectric materials convert heat into electricity, and it can change electrical energy to the cold. Good thermoelectric materials depend on their thermoelectric properties such as thermoelectric sensitivity, electrical characteristics, and thermal conductivity. Thermoelectric sensitivity is the charge carriers and Seebeck coefficient (S), which was determined using the hot probe method. Electrical characteristics were assessed from the electrical resistivity (ρ), it was measured by the standard four-probe method. The steady state technique is used to find the thermal conductivity (κ). The thermoelectric efficiency can be examined from the power factor ($P = S^2/\rho$) and figure of merit ($Z = S^2/\rho\kappa$). The performance of the thermoelectric materials is usually characterized in terms of their dimensionless figure of merit parameter ($ZT = S^2T/\rho\kappa$, where T is the absolute temperature)^[2]. The highest $ZT \approx 1.0$ has been achieved from the state of the art thermoelectric material Bi₂Te₃ and Sb₂Te₃ at room temperature^[3,4]. Both theoretical and experimental approaches have been conducted to search for new materials of higher ZT . This has been an important task in the development of

thermoelectric technology.

The search for new thermoelectric materials is important that the transition metal oxides were interested such as p-type Ca₃Co₄O₉^[5-10] and n-type CaMnO₃^[11-15]. They have been synthesized using different techniques in the form of powder and bulk. The thermoelectric properties and applications were further studied. However, the doped metals (Ag, Bi, Mo, La, etc.) have been expected the candidates for good thermoelectric materials, including thermoelectric module (TEM) consists of two or more materials of p-type and n-type^[16-18]. Recently, these thermoelectric devices (TED) are also being used as the thermoelectric generators, thermoelectric coolers, etc.^[19-20]. These are reasons of interest for the study and research. In this work, the p-Ca₃Co₄O₉ and n-CaMnO₃ bulks were made from powder precursors obtained from the conventional solid state reaction (SSR) method. A thermoelectric module was designed and constructed. The thermoelectric properties and efficiency were investigated.

EXPERIMENTAL PROCEDURES

A thermoelectric module was initially designed at the Physics Department, Loei Rajabhat University (LRU) and constructed at the Thermoelectric Research Center (TRC), Sakon Nakhon Rajabhat University (SNRU), Thailand. The details are described as follows.

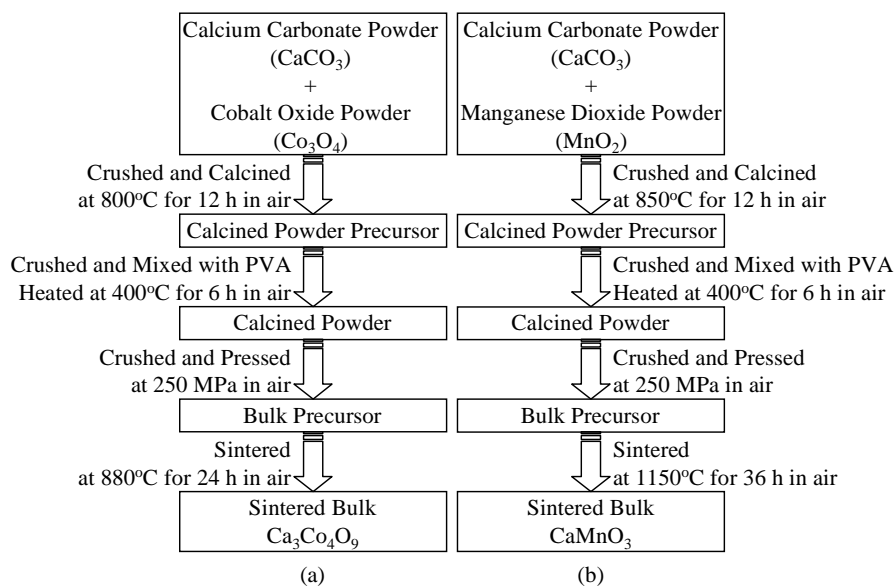
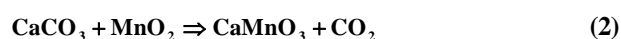
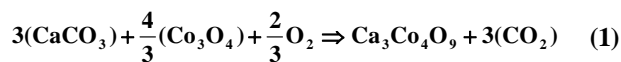


Figure 1 : Fabrication flow chart for the solid state reaction procedures used to prepare the polycrystalline samples of the Ca₃Co₄O₉ and CaMnO₃ thermoelectric oxides

Preparation of samples

The polycrystalline samples of $\text{Ca}_3\text{Co}_4\text{O}_9$ and CaMnO_3 thermoelectric oxides were made from powder precursors obtained from the solid state reaction method as summarized in Figure 1. These can be explained in Equation (1) and (2).



In the SSR method, calcium carbonate powder (CaCO_3 100.09 g/mol, ~99% purity, Sigma-Aldrich Co.) were separated and mixed with cobalt oxide powder (Co_3O_4 240.80 g/mol, 99.9% purity, Sigma-Aldrich Co.) and manganese dioxide (MnO_2 86.94 g/mol, 99.9% purity, Ajax Finechem Pty Ltd.) in molar ratios. Each of the mixed products were then crushed and calcined at 800°C and 850°C for 12 h in air, respectively. Both calcined powder precursors were then crushed and mixed with polyvinyl alcohol (PVA) in 1 g:1 mL ratios and heated at 400°C for 6 h in air. The calcined powders were then pressed into the bulk precursors at the pressure of 250 MPa in air before subjected to sintering stage. The bulks of $\text{Ca}_3\text{Co}_4\text{O}_9$ and CaMnO_3 were sintered at 880°C for 24 h and 1150°C for 36 h in air, respectively. Subsequently, the sintered bulks were cut and polished using the precision saw and grinder (IsoMet Low Speed Saw and MetaServ 3000, Buehler Ltd., USA) for determining thermoelectric properties and building module.

Determining thermoelectric properties

The cross-sectional area, length, and density of the $\text{Ca}_3\text{Co}_4\text{O}_9$ and CaMnO_3 bulks are given in TABLE 1. The determining thermoelectric properties at room temperature in air included the thermoelectric sensitivity, electrical characteristics, and thermal conductivity. The power factor and figure of merit were calculated. The thermoelectric properties were measured at the TRC using the built equipments which were already checked and compared with the calibration standard. The experimental setups can be elucidated as follows.

TABLE 1 : Cross-sectional area, length, and density of the samples

Samples	Cross-sectional area, A	Length, l	Density, ρ
$\text{Ca}_3\text{Co}_4\text{O}_9$	0.364 cm × 0.398 cm	0.700 cm	3.218 g/cm ³
CaMnO_3	0.356 cm × 0.382 cm	0.700 cm	2.862 g/cm ³

Firstly, the thermoelectric sensitivity can be considered from the type of charge carrier and Seebeck coefficient, which were determined by the hot probe method as shown in Figure 2. The hot and cold junctions between the across two ends of sample are connected to the digital multimeter (Fluke 73III). The hot (T_H) and cold (T_C) temperatures are sensed by the type K thermocouples (chromel-alumel). The resistor of 10 W, 5 Ω was used to heat the hot junction T_H by applying constant currents to the resistor placed on the hot side using the DC power supply (Model: GPS-3030D). Seebeck coefficient (S) was measured using the relation between thermoelectric voltage (ΔV) and the temperature difference ($\Delta T = T_H - T_C$), given by $S = \Delta V / \Delta T$ ^[21]. Secondly, the electrical characteristics were assessed from the electrical resistivity it was measured by the four-probe method^[22] as shown in Figure 3. All contacts were made by high purity silver paste (SPI Supplies and Structure Probe, Inc.), which showed ohmic characteristics over a wide range of currents. The DC power supply was used by applying the currents to the sample. The current-voltage characteristics for the measurement of electrical resistivity (ρ) are measured using the digital multimeter (Hewlett-Packard HP973A). The ρ of sample can be estimated by use of the equation, $\rho = RA/l$, where R is the resistance ($R = V/I$, V is the voltage, I is the current), A is the cross

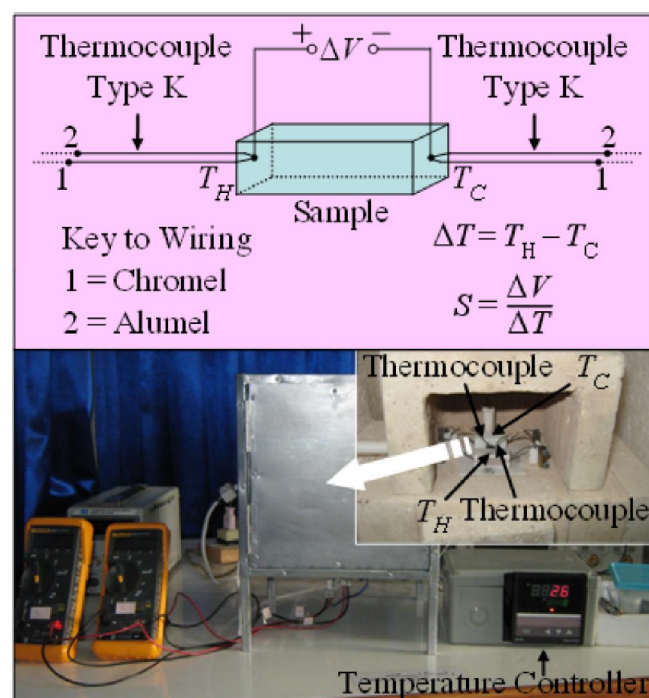


Figure 2 : Experimental setup of thermoelectric sensitivity

Full Paper

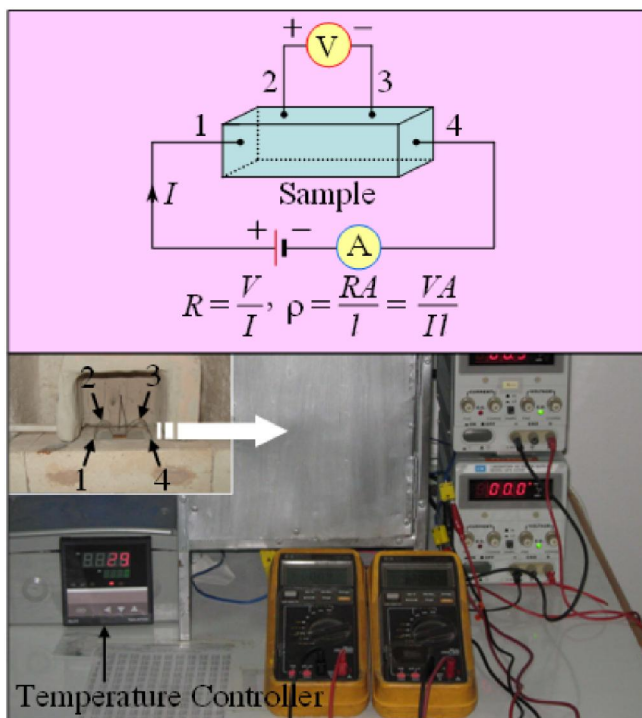


Figure 3 : Experimental setup of electrical characteristics

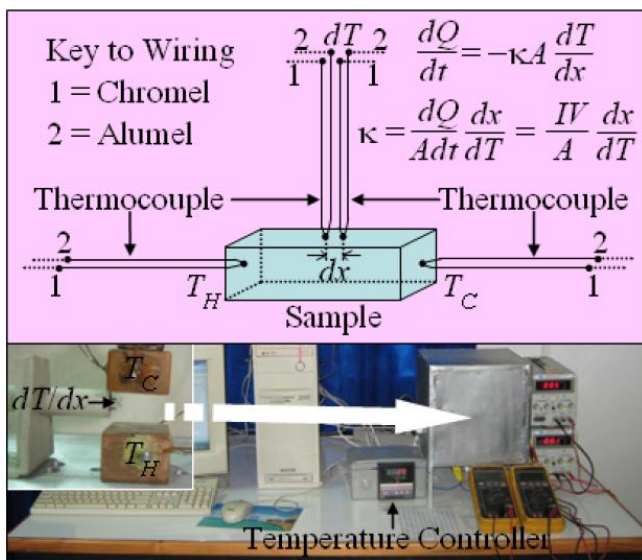


Figure 4 : Experimental setup of thermal conductivity

section, and l is the length of sample. Thirdly, the steady state technique is used to find the thermal conductivity (κ)^[21] as shown in Figure 4. The heat flow rate between two ends of the solids can be given as: $dQ/dt = -\kappa A (dT/dx)$ ^[23,24], where the rate of heat flow through a homogeneous solid ($dQ/dt = IV = PR$) is directly proportional to the cross-sectional surface area A , dT/dx is the temperature gradient along the path of the heat flow. The I and V is the voltage and current to the resistance R which was used to heat the hot junction by applying

constant currents to the resistor placed on the hot side using the DC power supply. The temperature difference (dT), the T_H and T_C are sensed by the type K thermocouples. Finally, the thermoelectric efficiency can be examined from the power factor (P) and figure of merit (Z). The P was calculated from the S and the ρ in the equation, $P = S^2/\rho$. The performance of the thermoelectric materials is usually characterized in terms of their figure of merit parameter, $Z = S^2/\rho\kappa$.

Design and construction of a thermoelectric module

A thermoelectric module fabricated in this study are composed of thirty-one p-n couples were designed and constructed using copper (Cu) electrodes and ceramic plates. Dimensions of $p\text{-Ca}_3\text{Co}_4\text{O}_7$ and $n\text{-CaMnO}_3$ bulks were 2.0 mm thick and high and 1.0 mm wide. The ceramic plates possessing dimensions 24.5 mm wide and long and 1.0 mm thick were used as substrate. The Cu sheets 1.0 mm in width, 2.0 mm length, and 0.05 mm in thickness were attached onto the ceramic plates using epoxy adhesive to maintain achieve electrical conduction. The p-n legs and Cu sheets on the ceramic plates were adhered by silver paint. The designed and constructed thermoelectric module is shown in Figure 5. The internal resistance (R_i) of the module was measured. The preliminary test, the built device was used for thermoelectric power generation. The module was placed on a hot plate (T_H) to heat at 340-423 K. The

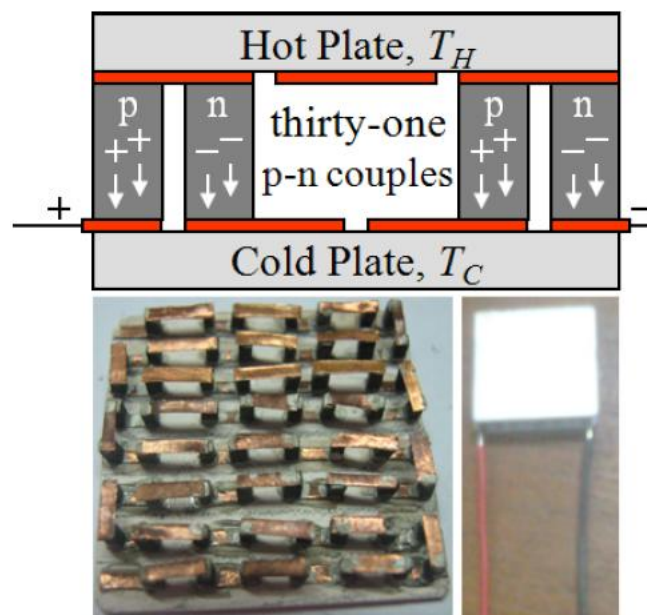


Figure 5 : The designed and constructed thermoelectric module

other side of the module was surrounded by air at room temperature (T_C). The temperature differences (T) and open circuit voltages (V_0) were measured.

RESULTS AND DISCUSSION

The determining thermoelectric properties of the $\text{Ca}_3\text{Co}_4\text{O}_9$ and CaMnO_3 bulks and the preliminary test on the thermoelectric module are given below.

Determining thermoelectric properties

The results of determining thermoelectric properties of bulk $\text{Ca}_3\text{Co}_4\text{O}_9$ and CaMnO_3 samples such as the type of charge carrier, Seebeck coefficient, electrical resistivity, thermal conductivity, power factor, and figure of merit are presented and discussed.

Firstly, charge carriers were determined by hot probe method (see Figure 2.). The result of measurement on $\text{Ca}_3\text{Co}_4\text{O}_9$ material, the cold junction shows higher voltage than the hot junction, indicating that the holes conduction dominated the transport properties (p-type). For CaMnO_3 ceramics, the negative sign points to electrons as majority carriers (n-type). Namely, the hot junction shows higher voltage than the cold junction. The measurement results and relation between the thermoelectric

voltage and temperature difference are shown in TABLE 2 and Figure 6, respectively. From Figure 6, the bulk $\text{Ca}_3\text{Co}_4\text{O}_9$ and CaMnO_3 samples indicate linear dependence between the thermoelectric voltage and temperature difference, the S of 0.147 ± 0.004 mV/K and 0.493 ± 0.006 mV/K are obtained, respectively. Secondly, electrical characteristics were measured using the four-probe technique (see Figure 3.). The experimental results and current-voltage characteristics are shown in TABLE 3 and Figure 7, respectively. From Figure 7, the plots exhibit the good ohmic I - V characteristics. The ρ values obtained from these I - V plots are 0.099 ± 0.002 m Ω ·m for $\text{Ca}_3\text{Co}_4\text{O}_9$, and 0.125 ± 0.001 m Ω ·m for CaMnO_3 . Thirdly, thermal conductivity can be estimated from the steady state technique (see Figure 4.). The results and relation between the heat flux and temperature gradient are shown in TABLE 4 and Figure 8, respectively. These measurements give the κ values of 10.21 ± 1.35 W/m·K for $\text{Ca}_3\text{Co}_4\text{O}_9$, and 10.71 ± 1.19 W/m·K for CaMnO_3 . Finally, the power factor and figure of merit were calculated and summarized in TABLE 5. From this table, the results give the P values of 0.218 ± 0.016 mW/m·K² for $\text{Ca}_3\text{Co}_4\text{O}_9$, and 1.944 ± 0.063 mW/m·K² for CaMnO_3 . The Z values of bulk $\text{Ca}_3\text{Co}_4\text{O}_9$ and

TABLE 2 : Results of determining thermoelectric sensitivity of $\text{Ca}_3\text{Co}_4\text{O}_9$ and CaMnO_3 at room temperature in air

$\text{Ca}_3\text{Co}_4\text{O}_9$					CaMnO_3				
T_H (K)	T_C (K)	ΔT (K)	ΔV (mV)	S (mV/K)	T_H (K)	T_C (K)	ΔT (K)	ΔV (mV)	S (mV/K)
306.25	301.75	4.50	0.65	0.144	305.65	301.55	4.10	1.98	0.483
309.65	302.85	6.80	1.02	0.150	311.55	303.45	8.10	4.02	0.496
312.65	303.95	8.70	1.27	0.146	318.35	305.85	12.50	6.13	0.490
316.45	305.65	10.80	1.53	0.142	323.85	308.15	15.70	7.81	0.497
328.35	309.55	18.80	2.87	0.153	325.15	308.75	16.40	8.15	0.497

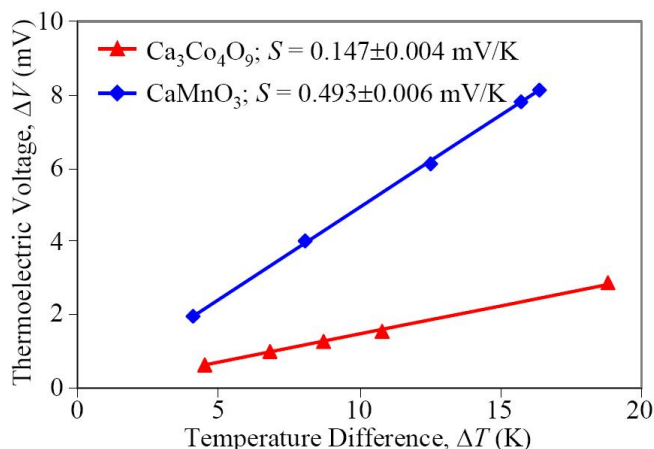


Figure 6 : Thermoelectric voltage of the bulk $\text{Ca}_3\text{Co}_4\text{O}_9$ and CaMnO_3 samples as a function of temperature difference

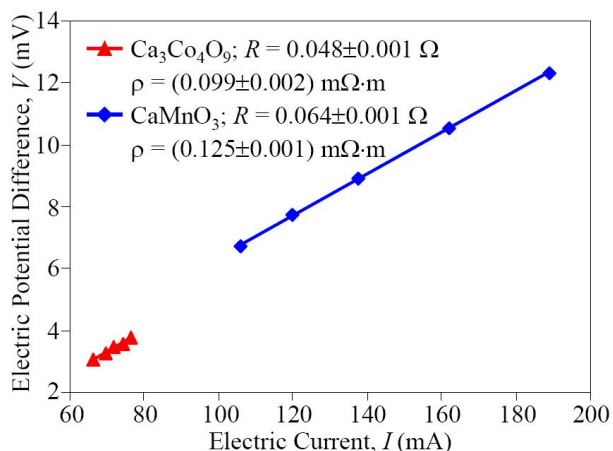


Figure 7 : I - V characteristic of the bulk $\text{Ca}_3\text{Co}_4\text{O}_9$ and CaMnO_3 samples for the measurement of electrical resistivity

Full Paper

TABLE 3 : Results of determining electrical characteristics of Ca₃Co₄O₉ and CaMnO₃ at room temperature in air

Ca ₃ Co ₄ O ₉				CaMnO ₃			
<i>I</i> (mA)	<i>V</i> (mV)	<i>R</i> (Ω)	ρ (mΩ·m)	<i>I</i> (mA)	<i>V</i> (mV)	<i>R</i> (Ω)	ρ (mΩ·m)
66.23	3.09	0.047	0.097	106.00	6.71	0.063	0.123
69.54	3.26	0.047	0.097	120.00	7.75	0.065	0.125
71.81	3.46	0.048	0.100	137.50	8.89	0.065	0.126
74.16	3.57	0.048	0.100	162.20	10.54	0.065	0.126
76.60	3.78	0.049	0.102	189.00	12.34	0.065	0.127

TABLE 4 : Results of determining thermal conductivity of Ca₃Co₄O₉ and CaMnO₃ at room temperature in air

Ca ₃ Co ₄ O ₉			CaMnO ₃		
<i>dT/dx</i> (K/m)	$(dQ/dt)/A$ (W/m ²)	κ (W/m·K)	<i>dT/dx</i> (K/m)	$(dQ/dt)/A$ (W/m ²)	κ (W/m·K)
259.26	2761.06	10.65	259.26	2941.35	11.35
407.41	3451.32	8.47	407.41	3676.69	9.02
518.52	6212.38	11.98	555.56	6618.04	11.91
777.78	7247.78	9.32	777.78	7721.04	9.93
1037.04	11044.23	10.65	1037.04	11765.40	11.35

TABLE 5 : *S*, ρ , *P*, and *ZT* of Ca₃Co₄O₉ and CaMnO₃ at room temperature in air

Samples	<i>S</i> (mV/K)	ρ (mΩ·m)	κ (W/m·K)	<i>P</i> (mW/m·K ²)	<i>Z</i> ($\times 10^{-3}$ K ⁻¹)
Ca ₃ Co ₄ O ₉	0.147±0.004	0.099±0.002	10.21±1.35	0.218±0.016	0.021±0.004
CaMnO ₃	0.493±0.006	0.125±0.001	10.71±1.19	1.944±0.063	0.182±0.026

Preliminary test on the thermoelectric module

The result of test on a p-Ca₃Co₄O₉/n-CaMnO₃ thermoelectric module and relation between the open circuit voltage and temperature difference are shown in TABLE 6 and Figure 9, respectively. The result shows linear dependence between the thermoelectric voltage and temperature difference. The *V*₀ values increase with temperature from 20 mV at *T*_H = 340 K and *T*_C = 306 K to 50 mV at *T*_H = 423 K and *T*_C = 343 K in air. The *R*₁ of module reached a value of 968.45 kΩ.

TABLE 6 : *T*_H, *T*_C, ΔT , and *V*₀ of the p-Ca₃Co₄O₉/n-CaMnO₃ thermoelectric module

<i>T</i> _H (K)	<i>T</i> _C (K)	$\Delta T = T_H - T_C$	<i>V</i> ₀ (mV)
340.15	306.65	33.50	20.00
342.15	308.15	34.00	22.00
352.15	309.65	42.50	27.00
363.15	314.15	49.00	29.00
373.15	318.15	55.00	33.40
393.15	324.15	69.00	44.00
423.15	343.15	80.00	50.00

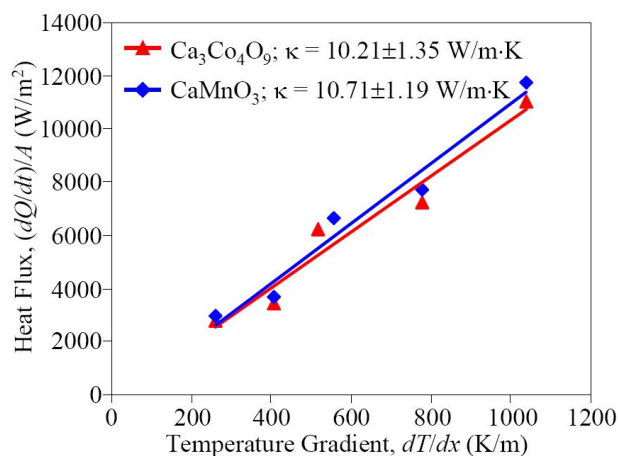


Figure 8 : Heat flux of the bulk Ca₃Co₄O₉ and CaMnO₃ samples as a function of temperature gradient

CaMnO₃ samples are $(0.021 \pm 0.004) \times 10^{-3}$ K⁻¹ and $(0.182 \pm 0.026) \times 10^{-3}$ K⁻¹, respectively. However, both bulks showed the low *S*, high ρ , and large κ , which led to the low *P* and *Z*, expecting that the samples have low densities and non-metal doping.

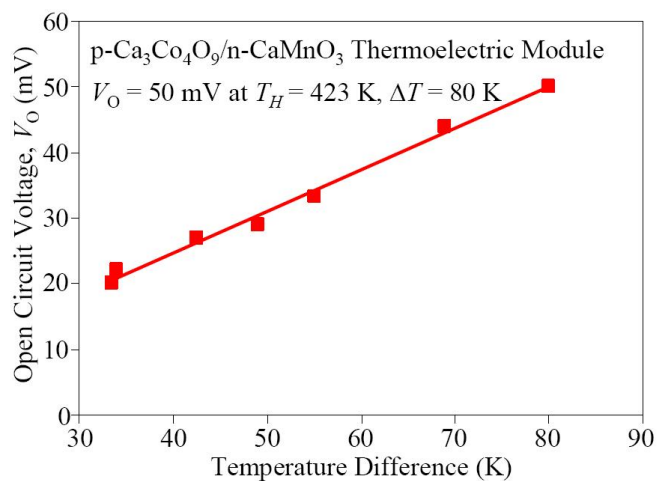


Figure 9 : Open circuit voltage of the p-Ca₃Co₄O₉/CaMnO₃ thermoelectric module as a function of temperature difference

CONCLUSIONS

The polycrystalline samples of p-Ca₃Co₄O₉ and n-CaMnO₃ thermoelectric oxides can be successfully prepared using the solid state reaction method. The measurement of thermoelectric properties showed the low

Seebeck coefficient, high electrical resistivity, and large thermal conductivity, which lead to the low power factor and figure of merit. The designed and constructed of an oxide thermoelectric device can be used for electrical power generation. This device could generate up to 50 mV of open circuit voltage at hot-side temperature of 423 K and cold-side temperature of 343 K. The internal resistance of the module reached a value of 968.45 k Ω . However, the module built could be used to generate low thermoelectric power. The doped metals have been expected to be one of the candidates for good thermoelectric generators. This will be further investigated.

ACKNOWLEDGEMENT

This work was financially supported by the Research and Development Institute, Loei Rajabhat University. Asst.Prof.Dr.Tosawat Seetawan, the Thermoelectric Research Center, Sakon Nakhon Rajabhat University are gratefully acknowledged for the preparation of the samples, construction of thermoelectric module, measurement of thermoelectric properties, and test on the thermoelectric module. The National Metal and Materials Technology Center is acknowledged for the XRD analysis.

REFERENCES

- [1] A.Hamburg; Analysis of Energy Development Perspectives. Doctor of Philosophy in Power Engineering and Geotechnology, Department of Electrical Power Engineering, Faculty of Power Engineering, Tallinn University of Technology, (2010).
- [2] J.H.Goldsmith; Thermoelectric Refrigeration. New York: Plenum Press, (2005).
- [3] H.Wang, W.D.Porter, J.Sharp; International Conference on Thermoelectrics, Dallas, Texas: IEEE, 91-94 (2005).
- [4] L.M.Goncalves, C.Couto, P.Alpuim, D.M.Rowe, J.H.Correia; Sensors and Actuators A, **130-131**, 346-351 (2006).
- [5] A.C.Masset, C.Michel, A.Maignan, M.Hervieu, O.Toulemonde, F.Studer, B.Raveau, J.Hejtmanek; Physical Review B, **62(1)**, 166-175 (2000).
- [6] Y.Zhou, I.Matsubara, S.Horii, T.Takeuchi, R.Funahashi, M.Shikano, J.Shimoyama, K.Kishio, W.Shin, N.Izu, N.Murayama; Journal of Applied Physics, **93**, 2653-1658 (2003).
- [7] P.Limelette, V.Hardy, P.Auban-Senzier, D.J erome, D.Flahaut, S.H ebert, R.Fr esard, Ch.Simon, J.Noudem, A.Maignan; Physical Review B, **71**, 233108-1-4 (2005).
- [8] Y.Liu, Y.Lin, Z.Shi, C.W.Nan, Z.Shen; Journal of the American Ceramic Society, **88(5)**, 1337-1340 (2005).
- [9] Y.Song, C.W.Nan; Journal of Sol-Gel Science and Technology, **44**, 139-144 (2007).
- [10] S.Katsuyama, Y.Takiguchi, M.Ito; Journal of Materials Science, **43(10)**, 3553-3559 (2008).
- [11] D.Flahaut, R.Funahashi, K.Lee, H.Ohta, K.Koumoto; International Conference on Thermoelectrics, Japan: IEEE, 103-106 (2006).
- [12] X.Y.Huang, Y.Miyazaki, T.Kajitani; Solid State Communications, **145**, 132-136 (2008).
- [13] J.W.Park, D.H.Kwak, S.H.Yoon, S.C.Choi; Journal of Alloys and Compounds, **487(1-2)**, 550-555 (2009).
- [14] Y.Wang, Y.Sui, H.Fan, X.Wang, Y.Su, W.Su, X.Liu; Chemistry of Materials, **21**, 4653-4660 (2009).
- [15] A.Kosuga, Y.Isse, Y.Wang, K.Koumoto, R.Funahashi; Journal of Applied Physics, **105**, 093717-1-6 (2009).
- [16] I.Matsubara, R.Funahashi, T.Takeuchi, S.Li, K.Ueno, S.Sodeoka; The 19th International Conference on Thermoelectrics, Osaka, Japan, from <http://staff.aist.go.jp/funahashi-r/ICT2000-Mats.pdf>, October 22, (2010).
- [17] R.Funahashi, S.Urata, T.Mihara, N.Nabeshima, K.Iwasaki; Advances in Science and Technology, **46**, 158-167 (2006).
- [18] S.Urata, R.Funahashi, T.Mihara, A.Kosuga, S.Sodeoka, T.Tanaka; International Journal of Applied Ceramic Technology, **4(6)**, 535-540 (2007).
- [19] Pacific Supercool Ltd.; TEC Modules. from <http://www.thermoelectricsupplier.com/tec-modules.php>, October 22, (2010).
- [20] TE Technology, Inc.; Thermoelectric Modules. from http://www.tetech.com/?gclid=CPuz-7_xs6QCFQIB6wodmnSt0g, October 22, (2010).
- [21] G.S.Nolas, J.Sharp, H.J.Goldsmid; Thermoelectrics Basic Principles and New Materials Developments. New York: Springer, (2001).
- [22] L.M.Le on-Rossano; American Journal of Physics, **65(10)**, 1024-1026 (1997).
- [23] J.B.Marion, W.F.Hornyak; General Physics with Bioscience Essays. 2nd Ed. New York: John Wiley & Sons, (1997).
- [24] A.J.Slifka; Journal of Research of the National Institute of Standards and Technology, **105**, 591-605 (2000).